Phase behavior of dense three-component ionic microemulsions and electrical conductivity in the lamellar phase

A. Di Biasio
Dipartimento di Matematica e Fisica, Università di Camerino, I-62032 Camerino, Italy

C. Cametti, P. Codastefano, and P. Tartaglia
Dipartimento di Fisica, Università di Roma La Sapienza, Piazzale Aldo Moro 2, I-00185 Roma, Italy

J. Rouch
Centre de Physique Moléculaire Optique et Hertzienne, Université Bordeaux I, 351 Cours de la Libération, 33405 Talence CEDEX, France

S. H. Chen
Department of Nuclear Engineering and Center for Materials Science and Engineering, Massachusetts Institute of Technology, Cambridge, Massachusetts 02139
(Received 11 November 1992)

An extended phase diagram for an ionic microemulsion system made of water, *n*-decane, and the ionic surfactant sodium-di-2 ethyl-hexyl sulfosuccinate is deduced from a very extensive set of electrical-conductivity and neutron-scattering measurements. This diagram shows high-temperature phase transitions that explain some original features previously not reported. Furthermore we propose a phenomenological model based on the solution of a Poisson-Boltzmann equation which accounts well for electrical conductivity data we obtain in the lamellar phase.

PACS number(s): 82.70.Kj, 64.70.−p, 05.20.−y

I. INTRODUCTION

A three-component ionic microemulsion system made of an ionic surfactant sodium-di-2 ethyl-hexyl sulfosuccinate (AOT), water, and *n*-decane has been known to show a large variety of physical phenomena upon varying the composition of the mixture and temperature. Among many of these, we may mention the critical phenomenon, percolation phenomenon, and nonexponential relaxation of droplet dynamics in dense microemulsions. The phase behavior of this ternary microemulsion system is sensitively dependent on the water-to-surfactant molar ratio $X = [H_2O]/[AOT]$. At room temperature and for X in the range 10–50, a large one-phase region exists in the phase diagram, known as a L_2 phase, where the microemulsion consists of water droplets coated by a surfactant monolayer dispersed in a continuous medium of decane. In the L_2 phase, the radius of the water droplets is directly proportional to X, as has been proven by neutron-scattering [1] and quasielastic-light-scattering experiments [2]. For $X = 40.8$, a consolute critical point has been observed for a volume fraction ϕ of the droplets around 0.098 at a temperature close to 39.98 °C. The critical dynamics of the microemulsion can be well accounted for by the standard mode-coupling theory, provided one makes use of the renormalized values of the critical indices. However, an unusual feature of this critical dynamics is the existence of a large background correction due to the quasimacroscopic size of the droplets [2]. Similar effects have also been observed in nonionic surfactant and water critical mixtures [3]. On the other hand, we have recently found well-defined percolation loci in the temperature–volume-fraction plane from extensive electrical-conductivity measurements. At a constant value of X, percolation loci extend from the vicinity of the critical point up to large volume fractions of the microemulsions ($\phi > 0.80$) [4]. The percolation line in the T-ϕ plane has been well accounted for by the Xu and Stell theory of percolation in probability [5] and very recently by a Baxter theory for adhesive hard spheres when an appropriate temperature dependence of the interaction parameters is used [6]. Above the percolation threshold and at high volume fractions ($\phi \geq 0.40$) a bicontinuous structure has been evidenced by the analysis of neutron-scattering data [7]. Upon a further increase of the temperature and for values of the volume fraction of the dispersed phase greater than 0.40, a lamellar phase has been observed and we have already published preliminary results for the electrical-conductivity behavior of the microemulsion in this domain [8]. Very recently Sheu *et al.* [9] and Kotlarchyk, Sheu, and Capel [10] have reported extensive sets of data obtained mainly from small-angle x-ray-scattering experiments which indicated a new L_3 phase existing around room temperature and volume fractions higher than 0.75. A strange feature in this microemulsion phase diagram was, however, the observation of an apparent cusp, for a volume fraction of the order of 0.42 and temperature around 50 °C, at the boundary between the one-phase–two-phase transition and the lamellar domain. The presence of this cusp was very difficult to understand in terms

of theories of phase transitions. Owing to this complexity, a more precise determination of the phase diagram of these microemulsions became necessary in order to elucidate some of the phenomena described above. The first aim of this paper is then to provide a more accurate phase diagram for microemulsions at $X = 40.8$. It shows high-temperature phase boundaries, deduced from very extensive electrical-conductivity measurements. The occurence of a lamellar phase (L_α phase) has been observed in a large domain of the phase diagram at rather high temperatures and volume fractions. This phase is visualized as made of regularly stacked oil-surfactant bilayers of a given thickness. The second aim of this paper is to propose a phenomenological model of conductivity that accounts rather well for the electrical-conductivity measurements we performed in the lamellar phase. Furthermore, our experimental results are also consistent with the presence of a multiply connected sponge phase (L_3 phase) very recently observed by Sheu and co-workers [9, 10] and we have been able to measure in this phase the percolation loci. Some results are also reported for different values of the molar ratio of water to surfactant, namely $X = 20$ and $X = 50$, that support our interpretation.

II. PHASE DIAGRAM

A. Experiment

The experimental techniques we used have already been reported in the literature [2–4, 8]. The electrical-conductivity measurements were carried out using a Hewlett-Packard impedance analyzer HP4192A, with a conductivity cell consisting of fixed-spacing stainless-steel plane parallel electrodes. The calibration of the cell was made by using liquids of known electrical conductivity and permittivity. The temperature of the cell was varied from 13 to 75 °C in steps of 0.25 °C and the overall accuracy of the temperature determination was 0.02 °C. Microemulsion were prepared from pure D_2O for neutron-scattering measurements and very low conductivity (lower than $10^{-4}\ \Omega^{-1}\,m^{-1}$) freshly prepared H_2O for electrical conductivity measurements. Normal decane and AOT have been purchased, respectively, from Sigma (purity $\geq$ 99%) and Fluka Chem. A.G. (purity $\geq$ 98%) and used without any further purification. We have to remark that it is rather difficult to prepare samples at volume fractions greater than 0.75. This is due to the fact that the surfactant AOT can only be dissolved in oil which in turn enters at a very low percentage into the composition of the system. This might explain some uncertainties in the phase diagram at very high temperature since we cannot be completely sure of a total dissolution of AOT. However, the freshly prepared samples do not show any significant decay even at high temperature and we have verified that all the measurements were well reproducible upon heating and upon cooling. Let us discuss now the main features of the phase diagram we deduced from our experimental results. The phase diagram in $T - \phi$ plane at $X = 40.8$ is shown in Fig. 1. In our notation ϕ denotes the sum of volume fractions of water and AOT.

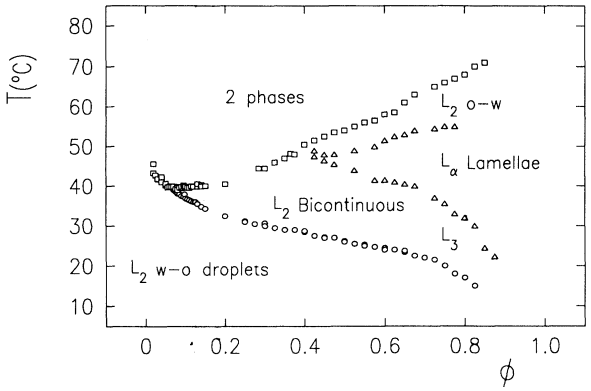

FIG. 1. Phase diagram of the water-decane-AOT microemulsion at $X = 40.8$.

B. L_2 water-in-oil droplet phase

Part of the phase diagram that extends from very low volume fractions ($\phi = 0.06$) up to volume fractions of the order of 0.30, has been previously reported in the context of the observation of the critical phenomenon [1, 2]. At least close to the critical point, the coexistence curve which shows a lower consolute critical point can be well described by the standard theory of critical phenomena with a value of the critical exponent $\beta = 0.33$ [2]. Below the coexistence curve, very extensive neutron-scattering experiments [11] clearly showed that the structure of the microemulsion system is made of water-in-oil (w-o) quasi-spherical droplets. Oil-in-water (o-w) droplets are present in a small region of the phase diagram. The radius of the water core is of the order of 60 Å, and the cores are coated by a monolayer of surfactant molecules. The droplets have size distribution and the polydispersity of the order of 30% is well described by a Schultz distribution [12]. The one-phase domain made of w-o quasispherical droplets is usually denoted by a L_2 phase. Above the phase-separation temperature T_p, equal to 39.98 °C at the critical volume fraction $\phi_c = 0.098$, the microemulsions separate into two microemulsion phases constituted by identical quasispherical w-o droplets but having different volume fractions [1]. This feature makes it possible to consider that the microemulsions behave like a pseudobinary mixture since the molar ratio X which governs the size of the droplets is a field variable in the sense of Griffiths and Wheeler theory [13] of critical phenomena in multicomponent systems. At low temperature and for not too high volume fractions, the electrical conductivity obeys the Eicke, Borkovec, and Das-Gupta [14] charge-fluctuation model, recently refined by Hall [15, 8]. Starting from volume fractions close to the critical one ϕ_c, we observed a characteristic percolative behavior of the microemulsion system (Fig. 2). The conductivity of the sample rises by typically six orders of magnitude upon heating. The percolation temperature, defined by the inflection point of conductivity versus the temperature plot, is shown as a function of the volume fraction by open circles also in Fig. 1. A good agreement between the percolation loci thus obtained and the contin-

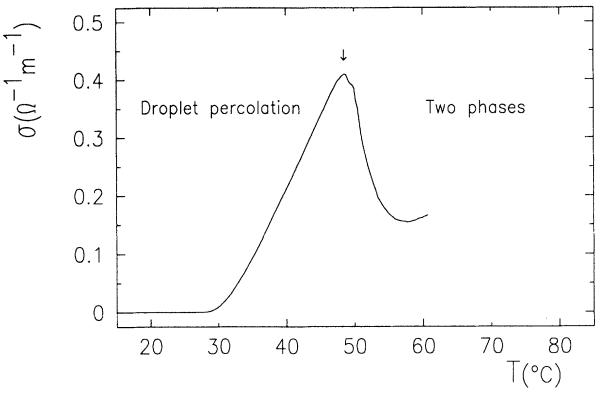

FIG. 2. Temperature dependence of electrical conductivity for $\phi = 0.375$. Below the maximum one observes the typical increase of the electrical conductivity with increasing temperature due to percolation. The conductivity suddenly changes when the system undergoes a phase separation and, with our experimental setup, it refers essentially to the oil-rich phase. The behavior is similar for any $\phi \leq 0.4$.

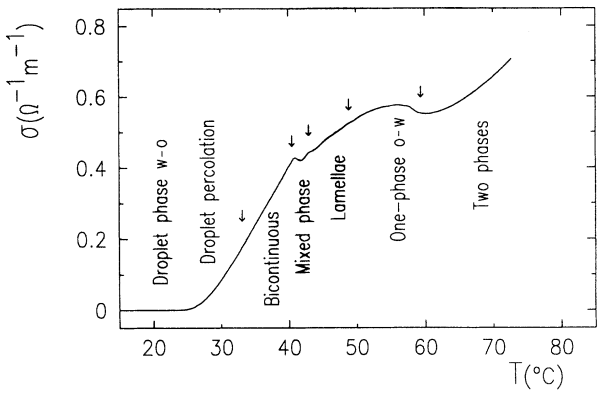

FIG. 3. Electrical conductivity for $\phi = 0.600$. The behavior is similar for any ϕ above 0.4 and is related to the various regions of the phase diagram annotated on the curve.

uum percolation theories has been demonstrated recently by us [4, 6, 8]. The mechanism of percolation below the threshold is the hopping of counterions within the fractal clusters formed due to a strong attraction between the droplets. Above the percolation threshold the microstructure of the microemulsions gradually transforms into a bicontinuous structure. This picture is consistent with the percolation indices we obtained below and above the percolation threshold [8]. Using the Xu and Stell theory for percolation in probability [5] and by assuming that the microemulsion droplets were interacting via a short-range repulsive hard-core potential followed with an attractive Yukawa tail with temperature-dependent parameters, we have been able to describe both the percolation loci and the coexistence curve qualitatively [4]. However, the experimental observation of the skewness of the coexistence curve (Fig. 1) was not accounted for by this model. In the case of binary solution of water and amphiphile, the skewness of the coexistence curve was attributed by Blanckstein, Thurston, and Benedek [16] to a polydispersity effect. However, very recently we used [6] Baxter's theory for monodisperse adhesive hard spheres [17] which gives a good description of both the percolation loci and of the coexistence curve. The great improvement of this analysis is the fact that the skewness of the coexistence curve appears as a natural consequence of Baxter's potential [6]. When the volume fraction is above $\phi = 0.40$, and in a temperature range corresponding to below the percolation threshold, the microemulsion is still made of w-o interacting quasi-spherical droplets. This shows a large extension in the phase diagram of the L_2 w-o droplet phase at least at low temperature.

C. L_2 bicontinuous structure

Above the percolation threshold and when the volume fractions of water and oil are not too different, i.e., for microemulsions whose volume fractions are larger than 0.40, we observe a rapid increase of the electrical conductivity to the level of conductivity of water upon heating the sample (Fig. 3). In the same domain of temperatures and volume fractions, the structure factor $S(Q)$ deduced from small-angle neutron-scattering experiments and depicted in Fig. 4 shows a characteristic broad peak at a certain value Q_M of the magnitude of the scattering vector. In this regime one can expect the microemulsion system to be constituted by interpenetrating water and oil microdomains. The bicontinuous microemulsion is then characterized by two length scales $d = 2\pi/k$ and ξ, the former one being the average separation between two water (or oil) domains and d/ξ is a measure of the polydispersity of the domain size [7]. A mathematical model for the structure factor containing the two length scales was proposed by Teubner and Strey [18] which was based on the Debye theory for porous media [19]. The structure factor $S(Q)$ that can be deduced from a small-angle neutron-scattering or an x-ray scattering experiment is

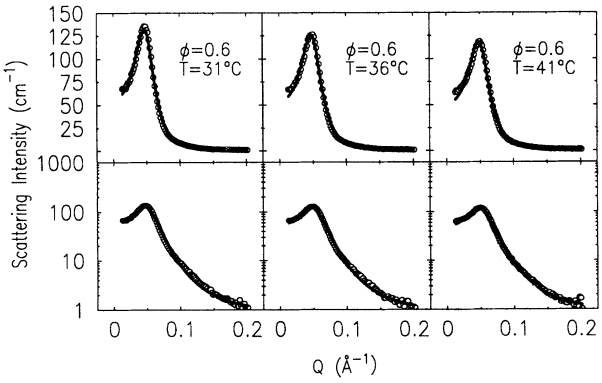

FIG. 4. The intensity of scattered neutrons $I(Q) = \langle \eta^2 \rangle S(Q)$, where $\langle \eta^2 \rangle$ is the scattering length density fluctuations vs amplitude of the scattering vector Q plotted in linear and logarithmic scales. The solid line is the fitted curve using the Teubner and Strey model given in Eq. (1).

given by

$$S(Q) = \frac{8\pi/\xi}{a^2 - 2Q_M^2 Q^2 + Q^4}, \quad (1)$$

where

$$a = k^2 + \frac{1}{\xi^2}, \quad Q_M^2 = k^2 - \frac{1}{\xi^2}. \quad (2)$$

A very good fit to our experimental results is obtained (full line in Fig. 4) with $k\xi \approx 2.70$, significantly larger than 2.0 generally observed for the disordered bicontinuous microemulsions [7]. This can be interpreted as signifying that the microemulsions are in an ordered bicontinuous state for temperatures above the percolation threshold approaching the lamellar phase boundary. One can consider the lamellar structure to be an extreme case of the ordered bicontinuous structure. The parameters used to fit the experimental data shown in Fig. 4 are reported in Table I.

D. Lamellar phase

Whereas upon heating the sample a continuous rapid increase of the electrical conductivity was observed in the bicontinuous phase, a sudden decrease appears, for instance, at a temperature of 40 °C for a volume fraction of 0.6 (see Fig. 3). Then, upon a further heating of the sample, again a slow but linear increase of the conductivity versus temperature is observed. This feature clearly indicates a phase transition. As we shall see below, we can interpret the domain of the phase diagram where the conductivity increases linearly with temperature as a lamellar phase. Then we can reasonably conjecture that the narrow domain of temperature where the conductivity is decreasing corresponds to a mixed phase consisting probably of coexisting lamellae and bicontinuous structures.

E. The two-phase domain. Does a cusp exist at $\phi = 0.40$?

At high temperature the linear increase in conductivity previously discussed is no longer observed. The electrical conductivity levels off, then decreases and rises again. The increase of the conductivity corresponds to the high-temperature two-phase domain. The boundary of this domain deduced from the inflection point of a σ vs T curve is shown by open squares in Fig. 1. It is clearly seen that the cusp previously reported was a result of an incomplete determination of the phase boundary. The two-phase boundary which is indicated by open squares is continuous and extends from low volume fractions to high volume fractions including the critical point. The existence of the so-called cusp would imply a junction between the one-phase–two-phase domain and the lamellar phase whose extent at this volume fraction is extremely narrow in temperature.

TABLE I. Teubner-Strey parameters [Eq. (1)] of the bicontinuous microemulsions.

$\phi = 0.6$	31 °C	36 °C	41 °C
k (Å^{-1})	0.0502	0.0512	0.0523
ξ (Å)	53.85	52.67	51.30
$k\xi$	2.70	2.69	2.68

F. L_3 phase

The high-volume-fraction part ($\phi > 0.75$) of the phase diagram very recently explored by Sheu *et al.* [9] and by Kotlarchyk, Sheu, and Capel [10] shows evidence of the occurrence of the L_3 phase around room temperature. The L_3 phase, which is optically isotropic at rest and birefringent upon a gentle stirring, is conjectured to have the same surfactant bilayer composition as the L_α phase but shows a multiply connected surface, as depicted by Strey *et al.* in Fig.2b of Ref. [20]. The results we infer from the electrical-conductivity measurements, which we have performed in this domain of the phase diagram, are consistent with the findings of Sheu *et al.* [9] and of Kotlarchyk, Sheu, and Capel [10]. We observed in fact a change of curvature of both the percolation line and of the boundary of the L_α phase. These lines show a sudden strong downward curvature. From our experiments in the highly conducting regime, we can infer the transition temperature from the L_3 to the L_α lamellar phase upon heating the sample as reported in Fig. 1. However, since the lowest temperature we can measure with our experimental setup is limited, we cannot deduce accurately the percolative behavior of the L_3 phase at very high volume fraction. Indeed the percolation temperature appears to be lower than the lower bound of our experiment.

III. ELECTRICAL CONDUCTIVITY IN THE LAMELLAR PHASE

Let us recall that at high volume fractions and for temperatures well above the percolation threshold, a structure consisting of repeated leaflets of water, surfactant, and oil, known as lamellar phases (L_α phase), is formed. Recent small-angle x-ray-scattering experiments have provided additional support for the evidence of the lamellar region [9, 10]. In this region of the phase diagram, the electrical-conductivity mechanism is completely different from that occuring in other molecular arrangements, both below and above the percolation. The ionic transport in this case is essentially due to the motion of the Na^+ ions derived from the ionization of the surfactant molecules within the water layers. Thus, in the lamellar-phase microemulsion, the electrical conduction reduces to a bulk phenomenon within the water region, the contribution of the other mechanism, i.e., the hopping of the AOT anions from one droplet to another or the opening of the surfactant layers to form extended water microchannels, being negligible. Within the region of existence of the lamellar phase, the structure of the microemulsion is made up of the alternate sequence of oil and water layers of constant thickness coated with a monomolecular layer of surfactant molecules, whose hydrophobic parts are fitted in an oil matrix.

Within this region, the properties of the water lamellae are independent of temperature. The thickness d_w of the water layer depends only on the molar ratio of water-to-surfactant X and is given by

$$d_w = \frac{2dXM_w\rho_{\mathrm{AOT}}}{M_{\mathrm{AOT}}\rho_w}, \tag{3}$$

whereas their repeat distance l depends on the composition through the fractional volume $\phi = \phi_w + \phi_{\mathrm{AOT}}$ according to the expression $l = (d_w + 2d)/\phi$. Here d is the length of an AOT molecule and M and ρ are the molecular weights and densities of water and surfactant. Moreover, each polar group of the surfactant molecule carries an electronic charge due to its ionization and consequently contributes one sodium ion to the water layer. The surface-charge density remains constant at the value $\sigma = 0.025$ C/m^2 corresponding to one charge per 61.8 Å^2, independent of the microemulsion composition. At $X = 40.8$ the water thickness is about $d_w = 39.5$ Å.

In the lamellar structure the polar head groups of the surfactant molecules are oriented towards the water phase and the conductivity is essentially due to ionic transport in a continuous medium, where the charge carriers are Na^+ ions and the medium is water. Their ionization produces a surface charge and Na^+ counterions dissolved in the water, giving rise to the formation of an electric double layer whose extension within the aqueous phase influences the electrical conductivity. If the microemulsion, in this phase region, is considered as a set of large, randomly oriented multilamellae, the overall conductivity of the system, which must reflect the fact that the ionic transport is locally anisotropic, can be written, to a first approximation, as

$$\sigma = \frac{1}{3}\frac{\sigma_l\sigma_w}{\sigma_w(1-\phi_w)+\sigma_l\phi_w} + \frac{2}{3}(\sigma_l(1-\phi_w)+\sigma_w\phi_w), \tag{4}$$

where σ_l and σ_w are the conductivities of the oil layer coated by the surfactant molecule and the water layer, respectively, and ϕ_w the volume fraction of water. The above equation is a simplified version of the effective-medium theory, where the system is modeled as a collection of capacitors coupled in series. The conductivity σ_w of the water layer, depending on its orientation in the applied external electric field, must be associated with the nonuniform spatial ion distribution within the water layer, which can be calculated with the Poisson-Boltzmann equation. The most interesting consequence is that when conduction occurs in a narrow water layer, only a fraction of counterions contributes to the ionic conductivity, whereas a large fraction is immobilized in the vicinity of the charged groups by means of strong electrostatic interactions. According to the model we adopted, the ionic distribution within the water layer can be obtained from the Poisson-Boltzmann equation in planar geometry

$$\frac{d^2\psi}{dx^2} = -\frac{4\pi zen_\infty}{\epsilon}\exp\left(-\frac{ze\psi}{k_BT}\right), \tag{5}$$

where ψ is the electrostatic potential at x, ϵ the dielectric constant of the water phase, k_BT the thermal energy, ze the electric charge, $n_\infty = fn_0$ the ion concentration when the potential is set to zero, and n_0 the unperturbed ion concentration. Introducing the dimensionless variables

$$y = -ze\frac{\psi}{k_BT}, \quad \xi = \kappa_D x, \tag{6}$$

where

$$\frac{1}{\kappa_D} = \left(\frac{4\pi e^2z^2n_0}{\epsilon k_BT}\right)^{-1/2} \tag{7}$$

is the Debye screening length, the Poisson-Boltzmann equation becomes

$$\frac{d^2y}{d\xi^2} = fe^y \tag{8}$$

whose solution, with the boundary conditions $y = 0$ and $dy/d\xi = 0$ at $\xi = 0$, is given by

$$y = \ln\left(1 + \tan^2\sqrt{\frac{f}{2}}\xi\right). \tag{9}$$

The electroneutrality condition within the whole water layer yields the constant f through the relation

$$\sqrt{2f}\ \tan\left(\sqrt{\frac{f}{2}}\kappa_D\frac{d_w}{2}\right) = \kappa_D\frac{d_w}{2}. \tag{10}$$

Given y, one can then calculate the ion distribution

$$n(\xi) = zefn_0e^{y(\xi)} = \frac{zefn_0}{\cos^2\left(\sqrt{\frac{f}{2}}\xi\right)}. \tag{11}$$

For sufficiently small external applied electric field the electrical conductivity requires the knowledge of the current density passing through the sample, whose general expression is

$$\mathbf{J}(x,t) = e\sum_i z_in_i(x,t)\mathbf{v_i}(x,t) + \frac{1}{4\pi}\frac{d\mathbf{D}}{dt}, \tag{12}$$

where $\mathbf{v_i}$ is the ith ion drift velocity, n_i is the ion concentration, and $\mathbf{D}$ is the electric displacement. The first term is the true conduction current and the second one the displacement current.

As we have noted, owing to the local anisotropy of the sample reflecting the random distribution of the lamellae orientation, the conductivity must be evaluated in two extreme limits when the external field is perpendicular and parallel to the lamellae. In the first case, following De Lacey and Withe [21], in the low-frequency limit, the conductivity equation furnishes a contribution given by

$$\sigma_\perp = zef\frac{n_0}{N_A}\lambda(T), \tag{13}$$

where N_A is the Avogadro number and $\lambda(T)$ the temperature-dependent equivalent conductance of the ions. When the external electric field is parallel to the lamellar orientation, the totality of the counterions present in the water layer should, in principle, contribute to the conductivity. In this case, however, strong elec-

trostatic interactions between the charged groups on the surface of the surfactant layer and ions dissolved in water reduce the effective concentration of ions which participate in the conduction. For the sake of simplicity, we assume that counterions lying in a layer adjacent to the charged surface are firmly bound thus possessing a negligible mobility. It follows that the average concentration of the ions that contribute to transport is given by

$$\overline{n} = \frac{2}{\kappa_D d_w}\int_0^{\frac{1}{2}\kappa_D d_w - \eta} d\xi\, n(\xi) = \frac{2ze\sqrt{2f}n_0}{\kappa_D d_w}\tan\left[\sqrt{\frac{f}{2}}\left(\frac{\kappa_D d_w}{2} - \eta\right)\right] \quad (14)$$

and consequently the conductivity is given by

$$\sigma_{\parallel} = ze\frac{\overline{n}}{N_A}\lambda(T). \quad (15)$$

Here we have introduced a parameter η to take into account the hindering effect at the charged surfactant-water interface on the transport of the ionic charge. The limiting values of η, $\eta = 0$, and $\eta = \kappa_D d_w/2$ correspond to the extreme conditions where all the ions within the water layer behave as free or bound ions, respectively. In the limit $\sigma_l \ll \sigma_\perp$ and $\sigma_\parallel$, Eq. (4) reduces to $\sigma = 2\sigma_\parallel \phi_w/3$ and is given by

$$\frac{\sigma(T)}{\phi_w} = \frac{8\ z^2\ e^2\ \sqrt{2\ f}}{3\ S_0\ d_w\ N_A}\tan\left[\frac{f}{2}\left(\frac{\kappa_D\ d_w}{2} - \eta\right)\right] \times \frac{\lambda(T)}{\kappa_D d_w}, \quad (16)$$

where $S_0 = 2/(n_0 d_w)$ is the average interfacial area occupied by each surfactant molecule, carrying the ionic SO_3^- group.

The experimental values of the electrical conductivity of the microemulsion at $X = 40.8$, normalized to the volume fraction of water ϕ_w in the temperature range where the lamellar structure occurs for ϕ between 0.45 and 0.70, are shown in Fig. 5. The solid line represents the calculated values according to Eq. (16), assuming that each surfactant molecule contributes one Na^+ ion to the water layer and using for the equivalent conductance λ a value of 50.2 Ω^{-1} cm^2 equiv^{-1} at 25 °C, with the temperature dependence described by

$$\frac{1}{\lambda}\frac{d\lambda}{dT} = 2.44 \times 10^{-2}\,^{\circ}\mathrm{C}^{-1} \quad (17)$$

quoted in the literature for the Na^+ ion [22]. As it can be seen, a good agreement with the experimental data is found with the parameter η corresponding to a thickness of immobilized ions of the surfactant-water interface equal to 1.7 times the Debye screening length. In the present case, with X=40.8, we obtain d_w = 39.5 Åand $\kappa_D^{-1} \approx 3.6$ Å. This means that approximately 30% of the total number of ions must be considered strongly bound to the charged surface and they do not contribute to the conductivity. To further investigate this ionic conduction mechanism in confined structures where strong electrostatic interactions between counterions and fixed charges at the surfactant-water interface dominate, we have also measured the electrical conductivity of an AOT-water-decane microemulsion system with a water-to-surfactant molar ratio of $X = 20$ and $X = 50$, corresponding to the water-layer thickness of the lamellar phase of 19.4 Å and 48.5 Å, respectively. It must be noted that at these microemulsion compositions, especially for $X = 20$, the region of existence of the lamellar phase is not very well defined and it is more questionable to attribute a phase boundary between different structures to changes in the shape of the conductivity curve. Figure 5 also shows the normalized conductivity σ/ϕ_w in the two latter cases. The full lines represent the calculated value according to Eq. (16) with $\eta = 3.3$ for microemulsions with $X = 20$ and $\eta = 2.9$ for microemulsions with $X = 50$. These values give the thickness, in Debye-length units, of the layer adjacent to the charge surface where ions are immobilized. The agreement with the measured conductivities is remarkably good, for all the volume fractions we measured in the lamellar phase, considering the simple model we are using.

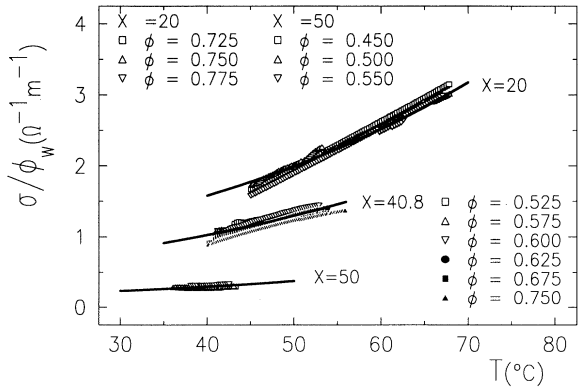

FIG. 5. The normalized conductivity for $X = 20$, 40.8, and 50. Each set of data represents the normalized conductivity for different values of ϕ where the lamellar phase occurs. The solid lines are calculated according to Eq. (16).

IV. CONCLUSIONS

From an extensive set of electrical-conductivity and neutron-scattering measurements, we have been able to deduce an extended phase diagram for a microemulsion system made of AOT, water, and decane. In particular, we have shown that the two-phase high-temperature domain is continuous extending from very low volume fractions up to high volume fractions, including the critical point. A bicontinuous structure has been evidenced for volume fractions greater than 0.40 and temperature above the percolation threshold. Our results also confirm the findings of Sheu *et al.* [9] showing the existence of a L_3 phase at high volume fraction ($\phi \geq 0.75$) and low temperature. We have been able to show evidence of a percolation line in this phase, at least at not too high volume fractions, where it goes to very low temperatures. Emphasis has been made in this work on the lamellar L_α phase. A theoretical model based on the so-

lution of the one-dimensional Poisson-Boltzmann equation gives values of the electrical conductivity in good quantitative agreement with the experiments. In particular, the scaling behavior of the electrical conductivity is very well obeyed for the microemulsion systems made with various values of the molar ratio X ranging from 20 to 50. As a final comment it is worth noting that these microemulsion systems which exhibit repeated bilayer-water structures are of fundamental biophysical interest. Indeed they serve as a simple model for biomembranes where the ionic conduction and transport may be investigated without the perturbative influence of proteins and other biomolecules which are usually embedded in the cell membrane. Moreover, the accumulation of ions close to charged surfaces in confined structures such as those investigated here can play an important role in determining functionality of pores and channels which govern the transport of ionic species through a membrane.

ACKNOWLEDGMENTS

This work has been supported by grants from the Ministero dell'Università e della Ricerca Scientifica e Tecnologica and the Gruppo Nazionale di Struttura della Materia del Consiglio Nazionale delle Ricerche, Italy. The Centre de Physique Moléculaire Optique et Hertzienne is "URA 283 du CNRS." The work of S.H.C. is supported by a grant from Materials Science Division of U.S. DOE.

[1] E. Y. Sheu, S. H. Chen, J. S. Huang, and J. C. Sung, Phys. Rev. A **39**, 5867 (1989); M. Kotlarchyk, S. H. Chen, J. S. Huang, and M. W. Kim, Phys. Rev. A **29**, 2054 (1984).

[2] J. Rouch, A. Safouane, P. Tartaglia, and S. H. Chen, J. Chem. Phys. **90**, 3756 (1989).

[3] J. Rouch, P. Tartaglia, A. Safouane, and S. H. Chen, Phys. Rev. A **40**, 2013 (1989).

[4] C. Cametti, P. Codastefano, P. Tartaglia, J. Rouch, and S. H. Chen, Phys. Rev. Lett. **64**, 1461 (1990).

[5] J. Xu and G. Stell, J. Chem. Phys. **89**, 1101 (1988).

[6] S. H. Chen, C. Y. Ku, J. Rouch, P. Tartaglia, C. Cametti, and J. Samseth, J. Phys. (Paris) (to be published).

[7] S. H. Chen, S. L. Chang, and R. Strey, Prog. Colloid Polym. Sci. **81**, 31 (1990); J. Chem. Phys. **93**, 1907 (1990); S. H. Chen, S. L. Chang, and R. Strey, J. Appl. Cryst. **24**, 721 (1991).

[8] C. Cametti, P. Codastefano, P. Tartaglia, J. Rouch, and S.H. Chen, Phys. Rev. A **45**, R5358 (1992).

[9] E. Y. Sheu, M. M. De Tar, M. Kotlarchyk, J. S. Lin, M. Capel, and D. A. Storm, in *Structure and Dynamics of Strongly Interacting Colloids and Supramolecular Aggregates in Solution*, edited by S. H. Chen, J. S. Huang, and P. Tartaglia (Kluwer Academic, Norwell, MA, 1992), Vol. 369.

[10] M. Kotlarchyk, E.Y. Sheu, and M. Capel, Phys. Rev. A **46**, 928 (1992).

[11] See a review article by S.H. Chen, T.L. Lin, and J.S. Huang, in *Physics of Complex and Supramolecular Fluids*, edited by S. Safran and N.A. Clark (Wiley, New York, 1987).

[12] M. Kotlarchyk and S. H. Chen, J. Chem. Phys. **79**, 2461 (1983).

[13] R. B. Griffiths and J. C. Wheeler, Phys. Rev. A **42**, 1047 (1970).

[14] H. F. Eicke, M. Borkovec, and B. Das-Gupta, J. Phys. Chem. **93**, 314 (1989).

[15] D. G. Hall, J. Phys. Chem. **94**, 429 (1990).

[16] D. Blanckstein, G. M. Thurston, and G. Benedek, J. Chem. Phys. **84**, 4558 (1986); **85**, 7268 (1986).

[17] R. J. Baxter, J. Chem. Phys. **49**, 2770 (1968); B. Barboy, *ibid.* **61**, 3194 (1974); Chem. Phys. **11**, 357 (1975).

[18] M. Teubner and R. Strey, J. Chem. Phys. **7**, 3195 (1987).

[19] See the review article by S. H. Chen and S. L. Chang, in *Structure and Dynamics of Strongly Interacting Colloids and Supramolecular Aggregates in Solution*, edited by S.H. Chen, J.S. Huang, and P. Tartaglia (Kluwer Academic, Norwell, MA, 1992), Vol. 369.

[20] R. Strey, W. Jahn, M. Skouri, G. Porte, J. Marignan, and U. Olsson, in *Structure and Dynamics of Strongly Interacting Colloids and Supramolecular Aggregates in Solution*, edited by S. H. Chen, J. S. Huang, and P. Tartaglia (Kluwer Academic, Norwell, MA, 1992), Vol. 369.

[21] E. H. B. De Lacey and L. R. White, J. Chem. Soc. Faraday Trans. **78**, 457 (1982).

[22] *American Institute of Physics Handbook*, 3rd ed. (McGraw-Hill, New York, 1977).